Chapter 2

OPTICAL COHERENCE TOMOGRAPHY

Through the understanding of optical coherence tomography (OCT), the fundamental limits of imaging performance can be identified. Within these limits functionality improvements can be identified to move beyond the capabilities of currently available OCT systems. It is important to determine the ability of OCT to adapt towards quantitative diagnostics for AMD progression.

2.1 Basics of Optical Coherence Tomography (OCT)

2.1.1 Michelson Interferometer with Single Wavelength Light Source

Optical coherence tomography is based upon a Michelson interferometer configuration. Consider a single wavelength narrow bandwidth laser source incident on a Michelson interferometer. The incoming light is split using a beamsplitter into two interferometer arms, designated as the reference and sample arms. The light is reflected back through the beamsplitter to be collected by the photodetector, which converts the measured power into an electrical current.

Looking at the complex form of the electric field of the laser light, the light traveling through the reference arm of the interferometer arrives at the detector has the form of $\widetilde{E}_R = E_R \exp(i(kz_{total,R} + \varphi_0))$, where $z_{total,R} = z_1 + 2z_R + z_4$ is the total optical path the light has traveled through the interferometer, φ_0 is phase of electric field of light source before it enters the interferometer, and $k=2\pi/\lambda$ for the light source of wavelength λ. Similarly, the electric field traveling through the sample arm of the interferometer is of the form $\widetilde{E}_S = E_S \exp(i(kz_{total,S} + \varphi_0))$, where $z_{total,S} = z_1 + 2z_S + z_4$ is the total optical path traveled in this case.

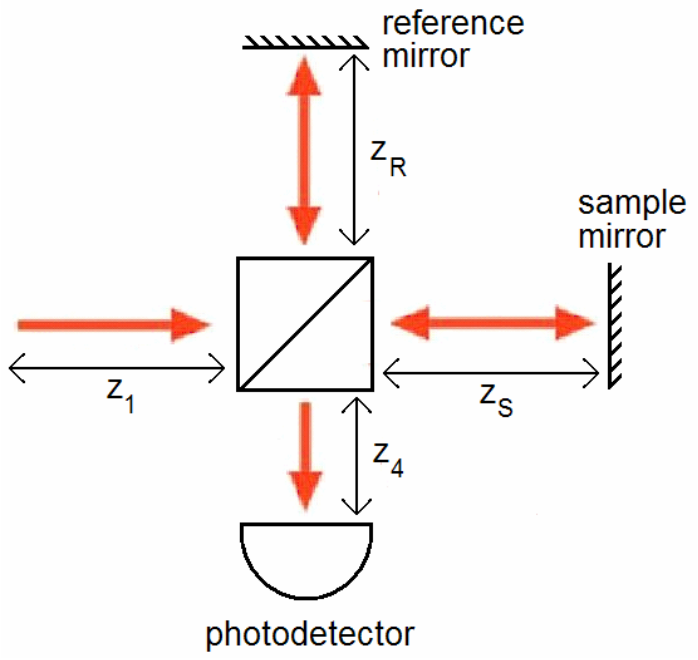

Figure 2.1: Free space Michelson interferometer with single reflector in each arm, designated as reference and sample.

The photodetector measures intensity of light, calculated by the magnitude of the total electric field arriving at the detector.

$$I_{Detector} = \left|\tilde{E}_S + \tilde{E}_R\right|^2 = \left|E_S \exp(i(kz_{total,S} + \varphi_0)) + E_R \exp(i(kz_{total,R} + \varphi_0))\right|^2$$

$$= {E_S}^2 + {E_R}^2 + 2E_S E_R \cos(kz_{total,S} + \varphi_0 - kz_{total,R} - \varphi_0)$$

$$= {E_S}^2 + {E_R}^2 + 2E_S E_R \cos(2k(z_S - z_R))$$

$$= I_S + I_R + 2\sqrt{I_S I_R}\cos(2k(z_S - z_R)) = I_{Detector}(k, z_S - z_R) \qquad (2.1)$$

where $I_S = \left|\tilde{E}_S\right|^2 = {E_S}^2$ and $I_R = \left|\tilde{E}_R\right|^2 = {E_R}^2$.

The interferometric signal measured only depends on relative optical path differences of the two interferometer arms.

2.1.2 Michelson with Broad Bandwidth Light Source

For a broad bandwidth light source, treat each wavelength component as an individual light source which does not interfere with any other wavelength than itself. Define $I_R = R_R I_0 S(k)$ and $I_S = R_S I_0 S(k)$, where S(k) is normalized spectral function of the light source, and R_a is percentage of original light intensity I_0 reaching the detector for light traveling through arm a. Assuming uniform efficiency of the detector over the light source spectra, the detector measures the sum of all light source contributions for all wavelengths. Calculating in terms of k-space:

$$I(z_S - z_R) = \int_k I_{Detector}(k, z_S - z_R)dk$$

$$= \int_k ((R_S I_0 + R_R I_0)S(k) + 2\sqrt{R_S R_R} I_0 S(k)\cos(2k(z_S - z_R)))dk$$

$$= (R_S + R_R)I_0 + 2\sqrt{R_S R_R} I_0 \int_k S(k)\cos(2k(z_S - z_R))dk \,. \qquad (2.2)$$

The function $\int_k S(k)\cos(2k(z_S - z_R)))dk$ is an autocorrelation of the light source spectra that is defined as the Weiner-Khinchin theorem (Fourier transform of the magnitude of the electric field). The coherence function, which will be defined as $f_C(z)$ and is centered around $z = z_S - z_R$, is a function which determines the effect on the interference signal when reflections from the two arms of the interferometer are not of equal path length.

The coherence length l_C is the quantitative metric of the spatial extent each interference reflection is measured over. This is defined as the full width half-maximum (FWHM) of the envelope of the spatial measurement of the coherence function. The coherence length describes the ability of the system to separate different interference reflections from each other.

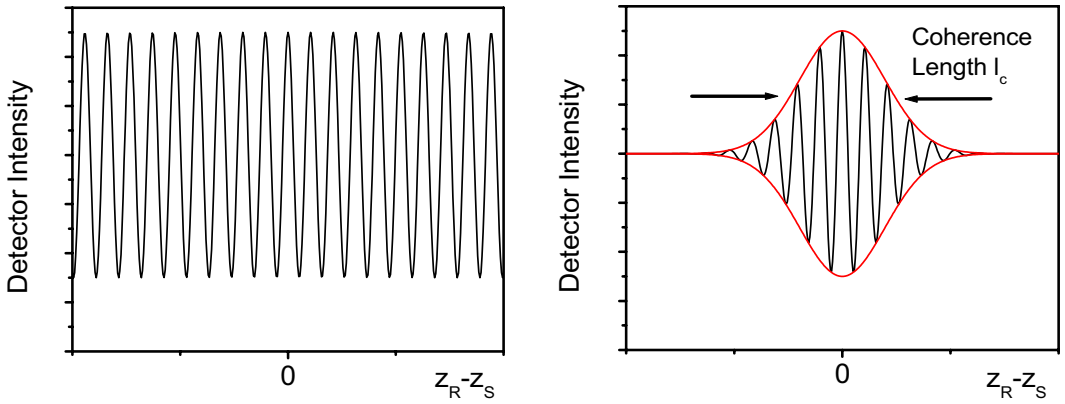

Figure 2.2: Measured light intensity at output of the Michelson interferometer as a function of the difference of the optical path lengths from the interferometer arms for the cases of single wavelength light (left) and broad bandwidth light (right). The full width half maximum (FWHM) of the interference fringe maximum is labeled as the coherence length.

2.1.3 Comparing Reflectivity to Interferometer Detector Signal

Consider the Michelson interferometer setup with a layered structure in the sample arm instead of a single reflector. The interference signal measured is the coherence function convoluted with the reflectivity profile of the sample.

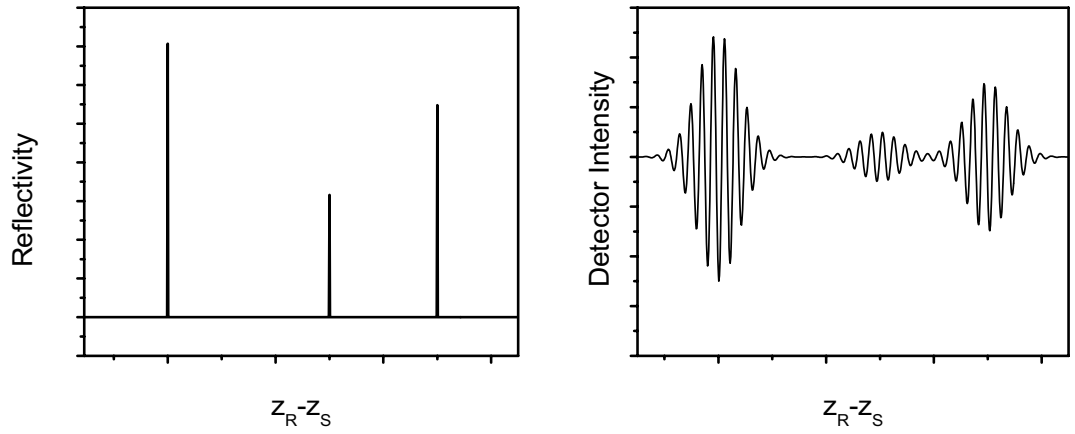

Figure 2.3: Ideal reflectivity profile over depth versus theoretical intensity signal over depth. The interference fringe signal is the convolution of the reflection profile with the coherence function.

2.2 Axial Resolution

The ability to separate fringes from reflections of different depths depends on the shape of the coherence function, which relies on the light source properties. This depth separation is referred to as the axial resolution. Consider the extreme cases:

a) For an infinitely narrow light source spectrum such that S(k)= $S_0 \delta(k_0)$,

$$f_C(z) = \int_k S(k)\cos(2k(z_S - z_R)))dk \propto \cos(2k_0(z_S - z_R))) . \quad (2.3)$$

In this case, interference fringes are observed for all $z_S - z_R$ values. All reflections from every depth within the same are observed all at the same time, resulting in the measurements being dominated by the strongest reflection.

b) For an infinitely broadband light source such that S(k)=1 for all k,

$$f_C(z) = \int_k S(k)\cos(2k(z_S - z_R)))dk \propto \delta(z_S - z_R) . \quad (2.4)$$

For this case, no interference would be observed unless the interferometer arms were of identical optical path lengths.

Spectral Shape and Coherence Function Tradeoffs

A finite-width broad bandwidth light source will measure interference over a spatial extent determined by the light source properties. The coherence function $f_C(z)$ contains the oscillatory interference fringe function based on the center wavelength of the light source combined with an envelope function which defines the spatial extent of the interference measurement. The coherence length l_C can be considered as the axial resolution, which determines the minimum depth difference at which two identical distinct reflections can be differentiated from each other.

For a Gaussian source spectra where the interferometer arm length difference is defined $z = z_S - z_R$, the coherence function $f_C(z) = \int_k S(k)\cos(2kz)dk$ can be calculated using the light source spectral form S(k) = S_0 exp(-4 ln 2 (k-k_0)^2/Δk_{FWHM}^2), where the spectrum is centered around $k_0=2\pi/\lambda_0$ and λ_0 is the center wavelength of the light source:

$$f_C(z) = \int_k S(k)\cos(2kz)dk = \mathrm{Re}\left(\int_k S(k)\exp(i2kz)dk \right)$$
$$= \mathrm{Re}\left(\exp(i2k_0 z) \int_{k'} S(k')\exp(i2k'z)dk' \right). \quad (2.5)$$

Using $S(k') = S_0 \exp(-C(k')^2)$, where $k' = k - k_0$ and $C = 4\ln 2 / \Delta k_{FWHM}{}^2$:

$$f_C(z) = \mathrm{Re}\left(S_0 \exp(i2k_0 z) \int_{k'} \exp(-Ck'^2)\exp(i2k'z)dk' \right)$$
$$= \mathrm{Re}\left(f_0 \exp(i2k_0 z)\exp(-z^2/C) \right)$$
$$= f_0 \cos(2k_0 z)\exp(-\Delta k_{FWHM}{}^2 z^2 / 4\ln 2). \quad (2.6)$$

In this case, the envelope function is a Gaussian function with a full width half maximum (FWHM) of $\Delta z_{FWHM} = 4\ln 2 / \Delta k_{FWHM} = l_C$. Defining the coherence length l_C in terms of wavelength uses $\Delta k_{FWHM} = \left(2\pi / \lambda_0{}^2 \right) \Delta\lambda_{FWHM}$ to calculate:

$$l_C = \frac{2\ln 2}{\pi} \frac{\lambda_0{}^2}{\Delta\lambda_{FWHM}} = 0.44 \frac{\lambda_0{}^2}{\Delta\lambda_{FWHM}}. \quad (2.7)$$

For the given light source bandwidth from the above equation, maximizing FWHM of the light source should produce the best axial resolution. Consider a top-hat spectra centered around k_0 with spectral width Δk_{FWHM}:

$$f_C(z) = \int_k S(k)\cos(2kz)dk = S_0 \int_{k_0-\Delta k_{FWHM}/2}^{k_0+\Delta k_{FWHM}/2} \cos(2kz)dk$$

$$= f_0 \cos(2k_0 z)\frac{\sin(\Delta k_{FWHM} z)}{\Delta k_{FWHM} z}, \tag{2.8}$$

which leads to a coherence length of:

$$l_C = \frac{3.79}{\Delta k_{FWHM}} = 0.60\frac{\lambda_0^{\,2}}{\Delta\lambda_{FWHM}}. \tag{2.9}$$

To compare these coherence length calculations directly, consider the case of the top-hat spectrum and the Gaussian spectrum with similar spectral extent such that $\Delta\lambda_{FWHM,Tophat} = 2\Delta\lambda_{FWHM,Gaussian} = 2\Delta\lambda_{FWHM}$, as shown in Figure 2.4.

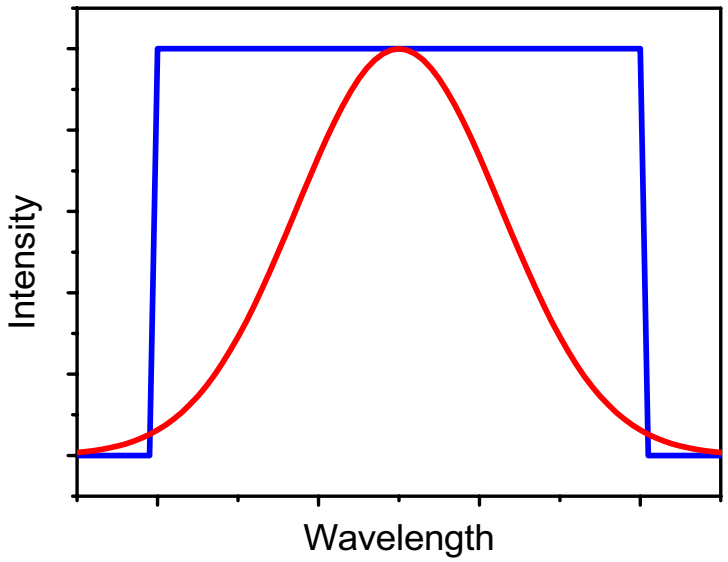

Figure 2.4: Plots of Gaussian (red) and top-hat (blue) spectral functions for the case of $\Delta\lambda_{FWHM,Tophat} = 2\Delta\lambda_{FWHM,Gaussian} = 2\Delta\lambda_{FWHM}$.

In this case, the top-hat source coherence function is $l_{C,Tophat} = 0.30\frac{\lambda_0^{\,2}}{\Delta\lambda_{FWHM}}$, and the Gaussian source coherence function is $l_{C,Gaussian} = 0.44\frac{\lambda_0^{\,2}}{\Delta\lambda_{FWHM}} = 1.47(l_{C,Tophat})$.

The coherence length l_C cannot be considered as the only important factor to consider. With the typical sample containing reflections that vary over several orders of magnitude, the spatial form of the coherence function determines how the weaker reflections are identified when located close to a strong reflection. If all of the reflections were identical within a sample, this would not be a consideration.

The interference signal in OCT is defined by the magnitude of the envelope of the coherence function convoluted with the reflectivity profile of the sample over depth. So for a normalized OCT signal of a given reflector, the coherence length is defined by the width, defined by the -6dB points (as opposed to the -3dB points used for the FWHM of the coherence envelope). On a linear scale, the side lobe variations of the coherence function due to the top-hat spectra do not seem to have much of an effect. On a logarithmic scale, the side lobes of this function are significant and extend out spatially far beyond the coherence length. On this scale, the coherence function of the Gaussian source spectra can be seen to have a larger coherence length but without any side lobes.

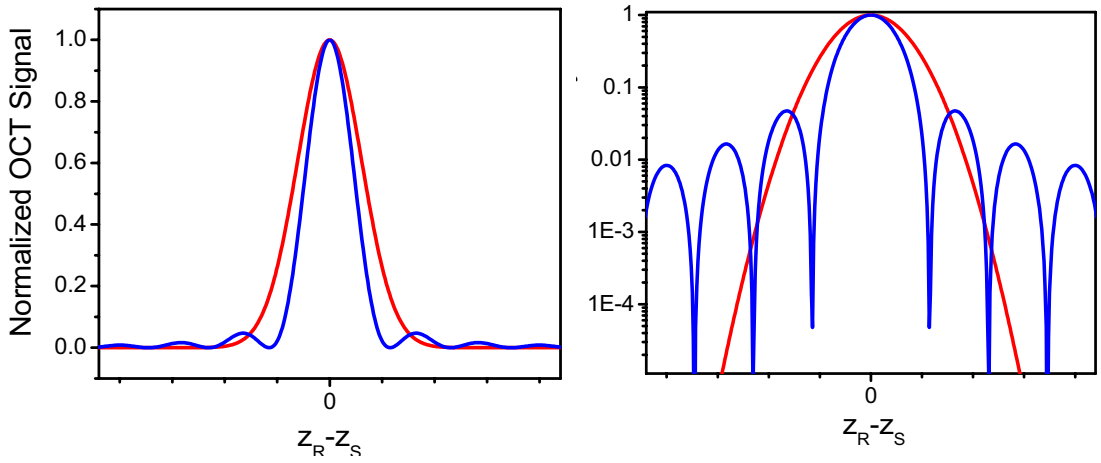

Figure 2.5: Calculated coherence functions of the spectra in Figure 2.4, plotted against the relative path length of the interferometer arm. The linear (left) and logarithmic (right) plots of the coherence functions are presented. The top-hat coherence function (blue) has a smaller coherence length, but has substantially more side lobes on the function. The Gaussian coherence function (red) shows no side lobes in either plot.

These two cases demonstrate the tradeoffs between coherence function shape and coherence length for a given source spectrum. The top-hat spectrum was the largest spectral FWHM for a given spectral width. The coherence length minimum for this given spectral width was at the tradeoff for the side lobes of the function. The coherence function created from the Gaussian spectra contains no side lobes, but has a relatively larger coherence length. Spectral shaping of the light spectrum allows adjustments between the coherence length and side lobes of the coherence function.

As illumination spectral widths become wider, dispersion compensation becomes more important. Dispersion mismatch between the interferometer arms causes a reflection to appear at different optical depths for different wavelength components of the light source, effectively broadening the coherence function and increasing the coherence length.

2.3 Acquiring Fringe Data to Create OCT Images

Optical coherence tomography (OCT) is the method of imaging which plots the spatial distribution of the envelope of interference fringes from a broad bandwidth light source in a Michelson interferometer configuration. The main question is: How is the envelope of the interference fringes determined?

For a single photodetector power measurement of an interference fringe, the measurement is of the form:

$$P(z_S - z_R) = P_{DC} + P_{INT} f_C(z_S - z_R)$$

$$= P_{DC} + P_{INT} f_E(z_S - z_R)\cos(2k_0(z_S - z_R))) \,. \qquad (2.10)$$

P_{DC} is the sum of all the powers measured by the photodetector, P_{INT} is the maximum power of the interference fringe, and $f_E(z)$ is the envelope function portion of the coherence function, normalized to a maximum of 1. The quantity of interest is $P_{INT} f_E(z_S - z_R)$, which is the non-normalized envelope function. The difficulty in

determining this factor from one detector measurement is due to two additional unknown variables beyond the quantity of interest: P_{DC} and $z_S - z_R$.

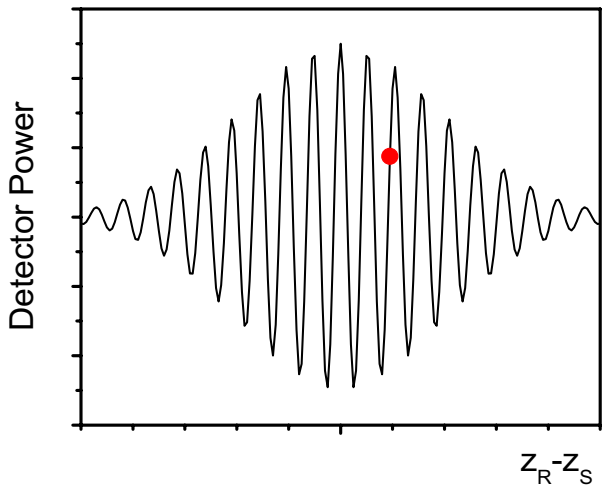

Figure 2.6: Schematic illustrating the lack of information for using a single point measurement to measure the interference fringe intensity.

The interferometric portion of the signal $\cos(2k_0(z_S - z_R))$ is very sensitive to the relative position $z_S - z_R$ of the two reflections. It is easier to consider this signal in terms of the relative phase $\phi_S - \phi_R$ of the interference fringe because, while the envelope function $f_E(z_S - z_R)$ is sensitive to distance changes on the order of microns, the fringe oscillation $\cos(2k_0(z_S - z_R))$ is sensitive to changes on the order of nanometers (1000 times more sensitive).

The relative phase of the interferometer $\phi_S - \phi_R$ is defined as $4\pi(z_S - z_R)/\lambda_0$, so any relative motion in the system with a magnitude of at least $\lambda_0/2$ will see a full oscillation in the interference fringe. By controlling the relative motion between the two arms of the interferometer, the fringe amplitude can be sampled and identified. The method of sampling the fringes through the change of interferometer optical path length is referred to as time domain optical coherence tomography (TDOCT) [1,2].

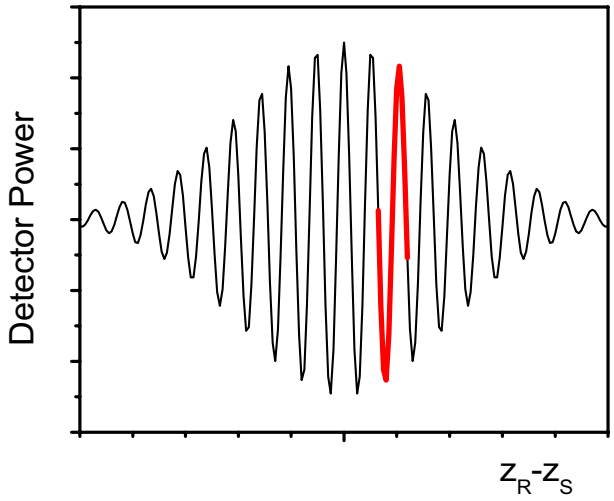

Figure 2.7: Schematic image of an interference fringe sampled using a small interferometer path length change.

There are several methods to sample the interference fringes to produce an OCT image. The most commonly used method utilizes a linear scan of the reference arm path length to sample all of the interference fringes over the entire depth of the sample. Keeping consistent with ultrasound scan terminology, a single scan along the depth of the sample is called an A-scan. Creating a two dimensional reflectance image through multiple A-scans over a range of transverse locations is called a B-scan.

As a screening tool for the retina, there is an additional interest in flexibility of the scan directions. Transverse images, also called en face images or C-scans, allow imaging at one depth of the interference fringes over the entire plane of the retina. If the primary acquisition of OCT data is through A-scans, the only way an en face image could be created would be through a 3D data set composed of A-scans measured over all transverse locations of interest. With mechanical scanning technologies limiting the maximum A-scan rate in TDOCT, it is not practical to produce transverse images this way.

To improve the flexibility of the imaging of the TDOCT system, the primary scan direction should be transverse to the direction of the incoming light (defined as axial). In this case, transverse scans followed by depth or axial scans would produce B-scan images.

Transverse scans followed by transverse scans in the perpendicular direction would produce C-scans. En face images are ideal in retinal imaging to screen an entire retina for signs of a disease, but allowing for it to occur at a single tissue depth of interest.

To acquire fringe information to allow for transverse scanning as the primary scan direction, the interference fringes must be sampled. The easiest way to sample requires changes in the relative optical path length much smaller than the axial resolution, which has numerous options available for creating small phase changes in the system at high speeds to measure the fringes [3-7].

2.4 SNR of Time Domain OCT

In TDOCT, the interferometric signal is measured as a current by the photodetector. Looking at the maximum fringe signal, the interferometer current i($z_S - z_R$) is given by:

$$i(z_S - z_R) = \frac{2\eta'\sqrt{P_R P_S}}{h\nu_0}\cos(2k(z_S - z_R)) \tag{2.11}$$

where η' is the quantum efficiency of the photodetector to convert photons to electrons. P_R, P_S are the powers arriving at the detector from the reference and sample arms of the interferometer, respectively and $h\nu_0$ is the average energy of the photon from the light source.

The signal in OCT $\mathrm{I(z)}^2$ is the spatial average of the square of the interferometer current over several fringes:

$$\mathrm{I(z)}^2 = \left\langle i(z)^2 \right\rangle_z = \frac{2\eta'^2 P_R P_S}{(h\nu_0)^2}. \tag{2.12}$$

The signal-to-noise ratio (SNR) in OCT is defined by the ratio of the OCT signal by the variance of the total noise of the system:

$$\mathrm{SNR} = \mathrm{I(z)}^2 / \sigma_{\mathrm{noise}}{}^2 . \tag{2.13}$$

There are three types of noise sources occurring over time τ' acquisition of a given pixel in the TDOCT acquisition: detector noise, shot noise, and relative intensity noise (which is also referred to as excess noise). The total noise in OCT is determined by the summation of the variance of all three types of noise sources:

$$\sigma_{\mathrm{noise}}{}^2 = \sigma_{\mathrm{detector}}{}^2 + \sigma_{\mathrm{shot}}{}^2 + \sigma_{\mathrm{excess}}{}^2 . \tag{2.14}$$

The detector noise can be considered a constant source of noise, independent of the amount of power incident on the detector.

$$\sigma_{\mathrm{detector}}{}^2 = \mathrm{constant} \tag{2.15}$$

Shot noise is defined by the statistical fluctuations which occur for the measure of a finite number of particles in a detector over a given amount of time. For electrical currents, the expected probability distribution for the number of electrons during the acquisition of the detector is given by a Poissonian distribution around the expected mean number of electrons. For this distribution, the variance of the measured electrons is equal to the mean number electrons measured within the time τ' of the detector, which is determined from the total power incident on the detector. For the case of $P_R >> P_S$, which is applicable for most OCT imaging scenarios, the shot noise variance is given by:

$$\sigma_{shot}{}^2 = \frac{\eta'(P_R + P_S)}{(h\nu_0)\tau'} \approx \frac{\eta' P_R}{(h\nu_0)\tau'} . \tag{2.16}$$

Relative intensity noise (RIN) describes the optical intensity fluctuation noise of the light source [8]. With the same assumption of $P_R >> P_S$:

$$\sigma_{excess}{}^2 = \left(\frac{\eta'(P_R + P_S)}{h\nu_0}\right)^2 \frac{\tau_{coh}}{\tau'} \approx \left(\frac{\eta' P_R}{h\nu_0}\right)^2 \frac{\tau_{coh}}{\tau'} . \tag{2.17}$$

In this equation τ_{coh} is the coherence time, defined by $\tau_{coh} = \left(\frac{2\ln 2}{\pi}\right)^{1/2} \frac{{\lambda_0}^2}{c\Delta\lambda_{FWHM}}$, where c is the speed of light, λ_0 is the center wavelength, and $\Delta\lambda_{FWHM}$ is the bandwidth of the light source.

Each of the different noise sources dominate in different regimes, which are determined by the total incident power on the detector, which is approximately described by P_R. From the properties of the individual noise sources and the OCT signal dependence on P_R, the ideal SNR performance would occur in the regime where the shot noise dominated the noise sources.

For the ideal SNR shot-noise limited case, given a TDOCT pixel acquisition time τ':

$$\mathrm{SNR_{TDOCT}} = \frac{2\eta'^2 P_R P_S/(h\nu_0)^2}{\eta' P_R/(h\nu_0)\tau'} = \frac{2\eta' P_S \tau'}{(h\nu_0)}. \tag{2.18}$$

2.5 Spectral Domain Optical Coherence Tomography (SDOCT)

Time domain optical coherence tomography (TDOCT) measures the interference in the case where a sample reflection has the same optical path length as the reference reflection. By measuring all of the interference fringes from all wavelength components at the same time within a photodetector, all of the non-equal path length fringes are rejected through destructive interference with each other.

The interference fringes have the form of $\cos(2k(z_S - z_R))$ for a given optical path difference of the interferometer arms of $z_S - z_R$. Measuring the interference fringes in k-space allows for the measurement of all of the interferometer fringes, not just the ones at equal path length. Each depth reflection will produce fringes of different spectral frequencies. The Fourier transform of the measurement of the interference fringes in k-space separates the reflections from different depths. This technique is referred to as Fourier domain optical coherence tomography (FDOCT) [9].

There are two different methods which fall under the category of FDOCT. The first method measures the interference fringes in k-space using a spectrometer to separate the wavelength components for measurement. This technique is called spectral domain optical coherence tomography (SDOCT) [10,11]. The other method utilizes a swept source laser with a narrow-band instantaneous spectral line width in the interferometer to vary the wavelength over time to be measured by a photodetector. This technique is referred to as swept source optical coherence tomography (SSOCT) or optical frequency domain imaging (OFDI) [12,13]. Regardless of the FDOCT method chosen, the calculation of the OCT signal from the spectral information remains the same.

Power measured in k-space for sample reflections (labeled by j, sample path locations z_j $=2(z_{Sj}-z_R)$ with reflected power labeled as P_{Sj}:

$$P(k)=P_R(k)+\sum_j P_{Sj}(k)+\sum_j 2\sqrt{P_R(k)P_{Sj}(k)}\cos(kz_j)$$
$$+\frac{1}{2}\sum_{\substack{i,j\\ i\neq j}} 2\sqrt{P_{Si}(k)P_{Sj}(k)}\cos(k(z_i-z_j)). \qquad (2.19)$$

For most scenarios $P_{Sj} << P_R$ which allows the last term to be ignored. By removing the DC component of the measured power signal ~ P_R (k), we are left with the approximate summation of all the sample reflections interfering with the reference reflection.

$$P(k)-P_R(k)\approx\sum_j 2\sqrt{P_R(k)P_{Sj}(k)}\cos(kz_j)$$
$$\approx\sum_j 2\sqrt{P_R P_{Sj}}S(k)\cos(kz_j) \qquad (2.20)$$

The function S(k) is the normalized spectral function of the light source defined earlier. Taking the Fourier transform of this interferometric signal in k-space allows the separation of the reflections from different depths:

$$FT(P(k)-P_R(k)) \approx \sum_j 2\sqrt{P_R P_{Sj}} \int_{-\infty}^{\infty} S(k)\cos(kz_j)\exp(ikz)dk\,. \qquad (2.21)$$

With the assumption that S(k) changes slowly relative to $\cos(kz_j)$, and making the assumption that $z_j=2(z_{Sj}-z_R) \geq 0$ simplifies the equation to:

$$\tilde{I}(z) = FT(P(k)-P_R(k)) \approx \sum_j \sqrt{P_R P_{Sj}} \int_{-\infty}^{\infty} S(k)\exp(ik(z-z_j))dk$$

$$= \sum_j \sqrt{P_R P_{Sj}}\,\tilde{f}_C(z-z_j)\,. \qquad (2.22)$$

$\tilde{f}_C(z-z_j)$ is the complex form of the coherence function derived earlier in this chapter such that Real[$\tilde{f}_C(z-z_j)$]= $f_C(z-z_j)$ and the amplitude of this function is the definition of the envelope of the coherence function. The signal in OCT is the magnitude of the Fourier transform of the interference signal in k-space:

$$\left|\tilde{I}(z)\right|^2 = \left|FT(P(k)-P_R(k))\right|^2 \approx \sum_j P_R P_{Sj}\left|\tilde{f}_C(z-z_j)\right|^2\,. \qquad (2.23)$$

The result is a summation of the magnitude of the envelope of the coherence functions centered around each of the sample reflection locations $z_j = 2(z_{Sj}-z_R)$, weighted by the power collected from each of the reflections P_{Sj}. This is identical to the form of the OCT signal measured in TDOCT.

One option available to SDOCT is the ability to adjust the coherence function through numerical spectral shaping. With the direct measurement of the spectral interference fringes, numerical shaping of the fringes before the Fourier transform is performed can alter the shape of the coherence function $f_C(z)$ and improve the coherence length while suppressing the side lobes.

For retinal imaging, the ideal method of FDOCT is not easy to determine. Only recently has there been developments of fast swept source lasers centered at wavelengths capable of retinal imaging (1300 nm light is absorbed too much while propagating through the 5cm of aqueous humor of the eye) [14,15,16]. High-speed line scan CCD cameras are readily available for incorporation into a spectrometer design [17,18,19]. For the extent of this project, SDOCT is chosen as the FDOCT method used for retinal imaging.

2.6 SNR of SDOCT

Define spectral domain optical coherence tomography (SDOCT) system, where the power from the reference arm arriving at the spectrometer is P_R and power from the sample arm arriving at the spectrometer is P_S. Assume that $P_S << P_R$. Integration time of the spectrometer is τ. The spectrometer has M pixels used in k-space measurements. Assume shot-noise-limited performance of the SDOCT system.

Number of electrons on CCD pixel in k-space:

$$F(k) = \sum_j 2S_j(k)\cos(kz_j + \phi_{Sj}) + F_{DC}(k) + N(k). \tag{2.24}$$

$S_j(k)$ is the interferometric signal is defined as $S_j(k) = \eta\sqrt{P_R(k)P_S(k)R_j}\,\tau / h\nu_0$ for a sample reflection R_j at optical path difference $z_j = 2(z_{Sj} - z_R)$ of interferometer. The summation of this signal is taken over all of the sample reflections. Define $P_R = \sum_k P_R(k)$, $P_S = \sum_k P_S(k)$.

$F_{DC}(k) + N(k)$ is the shot noise distribution of electrons. The mean number of electrons $F_{DC}(k)$ is given by $\eta P_R(k)\tau / h\nu_0$, where η is the combined light collection and electron conversion efficiency of the spectrometer for photons of energy $h\nu_0$. $N(k)$ is the random portion of the Gaussian distribution with variance $\sigma^2{}_{N(k)} = \eta P_R(k)\tau / h\nu_0$ and zero mean.

Using the property of the Fourier transform: $FT(A+B) = FT(A) + FT(B)$, the Fourier transform (FT) of F(k) produces the OCT intensity amplitude $\tilde{I}(z)$:

$$\tilde{I}(z) = FT(F(k)) = \sum_j FT(2S_j(k)\cos(kz_j + \phi_{Sj})) + FT(F_{DC}(k)) + FT(N(k)) \,. \quad (2.25)$$

Breaking it into the real and imaginary components of the complex Fourier transform of M data points in k-space:

$$\tilde{I}(z) = I(z)\exp(i\phi(z)) = FT(F(k)) = \sum_k^M F(k)\exp(-ikz)$$

$$= I_{\mathrm{Re}}(z) + iI_{\mathrm{Im}}(z) = \sum_k^M F(k)\cos(kz) - i\sum_k^M F(k)\sin(kz) \,. \quad (2.26)$$

Assume the number of data points in FT, defined as M, is large enough such that a delta function accounts for the Fourier transform of an oscillatory function. Let the arbitrary choice of $z_j \geq 0$ for all reflection locations be taken into account as well.

These assumptions lead to:

$$\sum_k^M \cos(kz)\cos(kz_j) = \sum_k^M \sin(kz)\sin(kz_j) = \frac{M}{2}\delta(z - z_j) \,, \; \sum_k^M \cos(kz)\sin(kz_j) = 0 \,. \quad (2.27)$$

DC Term

$$FT(F_{DC}(k)) = \sum_k^M F_{DC}(k)\exp(-ikz) \approx \delta(z)\sum_k^M F_{DC}(k) = \delta(z)\frac{\eta\tau}{h\nu_0}\sum_k^M P_R(k)$$

$$= \delta(z)\frac{\eta P_R \tau}{h\nu_0} \quad (2.28)$$

Interferometric Signal

Define the signal $\tilde{S}(z) = S(z)\exp(i\phi_S(z)) = \sum_k^M \sum_j 2S_j(k)\cos(kz_j + \phi_{Sj})\exp(-ikz)$. Using the identity $\cos(kz_j + \phi_{Si}) = \cos(kz_j)\cos(\phi_{Sj}) - \sin(kz_j)\sin(\phi_{Sj})$:

$$\widetilde{S}(z) = \sum_{k}^{M} \sum_{j} 2S_j(k)(\cos(kz_j)\cos(\phi_{Sj}) - \sin(kz_j)\sin(\phi_{Sj}))\exp(-ikz). \quad (2.29)$$

Assume $S_j(k)$ changes slowly compared to $\cos(kz_j)$ and $\sin(kz_j)$. With this assumption make the approximation within the summation: $\cos(kz)\cos(kz_j) = \sin(kz)\sin(kz_j)$ $= \frac{1}{2}\delta(z - z_j)$

$$\widetilde{S}(z) = \sum_{k}^{M} \sum_{j} 2S_j(k)(\cos(kz_j)\cos(kz)\cos(\phi_{Sj}) + i\sin(kz_j)\sin(kz)\sin(\phi_{Sj}))$$

$$= \sum_{k}^{M} \sum_{j=1} S_j(k)(\cos(\phi_{Sj}) + i\sin(\phi_{Sj}))\delta(z - z_j) = \sum_{j} \exp(i\phi_{Sj}) \sum_{k}^{M} S_j(k)\delta(z - z_j)$$

$$= \frac{\eta\tau}{h\nu_0} \sum_{j} \exp(i\phi_{Sj}) \sum_{k}^{M} \sqrt{P_R(k)P_S(k)R_j}\,\delta(z - z_j)$$

$$= \frac{\eta\sqrt{P_R P_S}\,\tau}{h\nu_0} \sum_{j} \exp(i\phi_{Sj})\sqrt{R_j}\,\delta(z - z_j) = S(z)\exp(i\phi_S(z)). \quad (2.30)$$

Noise Analysis

The noise calculated in OCT comes from the Fourier transform component of the noise distribution in k-space:

$$FT(N(k)) = \widetilde{N}(z) = N(z)\exp(i\phi_N(z)). \quad (2.31)$$

To understand how the noise transforms, Parseval's theorem for finite length Fourier transforms is required.

Using $\widetilde{f}(z) = \sum_{k}^{M} f(k)\exp(-ikz)$, where f(k) is a real function such that $(f(k))^* = f(k)$:

$$\sum_{z}^{M} \widetilde{f}(z)(\widetilde{f}(z))^* = \sum_{z}^{M} \widetilde{f}(z) \sum_{k}^{M} f(k)\exp(ikz)$$

$$\sum_z^M \left|\widetilde{f}(z)\right|^2 = \sum_k^M f(k) \sum_z^M \widetilde{f}(z)\exp(ikz) = \sum_z^M \sum_k^M f(k)\exp(ikz) \sum_{k'}^M f(k')\exp(-ik'z)$$

$$= \sum_k^M f(k) \sum_{k'}^M f(k') \sum_z^M \exp(i(k-k')z)$$

$$\sum_z^M \left|\widetilde{f}(z)\right|^2 = M \sum_k^M f(k) \sum_{k'}^M f(k')\delta(k-k') = M \sum_k^M \left|f(k)\right|^2 . \tag{2.32}$$

This theorem is important for relating the Fourier transforms of the shot noise distribution in k-space N(k), measured on the CCD. With $\widetilde{N}(z) = N(z)\exp(i\phi_N(z)) = \sum_k^M N(k)\exp(ikz)$:

$$\sum_z^M \left|\widetilde{N}(z)\right|^2 = M \sum_k^M \left|N(k)\right|^2 . \tag{2.33}$$

With the definition for the mean variation over all k-space measured as $\langle N(k)\rangle = 0$:

$$\sum_z^M \left|\widetilde{N}(z)\right|^2 = M\left\langle \left|\widetilde{N}(z)\right|^2 \right\rangle_z = M \sum_k^M \left|N(k)\right|^2 = M^2 \left\langle \left|N(k)\right|^2 \right\rangle_k = M^2 \left\langle \sigma^2{}_{N(k)} \right\rangle_k \tag{2.34}$$

$$\left\langle \left|\widetilde{N}(z)\right|^2 \right\rangle_z = M\left\langle \sigma^2{}_{N(k)} \right\rangle_k = \frac{\eta\tau}{h\nu_0} M\left\langle P_R(k)\right\rangle_k = \frac{\eta P_R \tau}{h\nu_0} \tag{2.35}$$

$$\widetilde{N}(z) = N(z)\exp(i\phi_N(z)) = N_{\mathrm{Re}}(z) + iN_{\mathrm{Im}}(z) . \tag{2.36}$$

Each component of Fourier Transform of random Gaussian noise distribution results in a Gaussian distribution as well. The real and imaginary components $N_{Re}(z)$, $N_{Im}(z)$ of the Fourier transform of the noise distribution N(k) are random Gaussian distributions, all centered around zero mean such that $\langle N(k)\rangle = \langle N_{\mathrm{Re}}(z)\rangle = \langle N_{\mathrm{Im}}(z)\rangle = 0$. With each component being independent of each other, the phase of the noise $\phi_N(z)$ is completely random. Determining the properties of the noise components:

$$\left|\widetilde{N}(z)\right|^2 = N_{\mathrm{Re}}(z)^2 + N_{\mathrm{Im}}(z)^2 \tag{2.37}$$

$$\left\langle \left|\widetilde{N}(z)\right|^2 \right\rangle = \left\langle N_{\mathrm{Re}}(z)^2 \right\rangle + \left\langle N_{\mathrm{Im}}(z)^2 \right\rangle = \sigma_{N\mathrm{Re}}{}^2 + \sigma_{N\mathrm{Im}}{}^2 . \tag{2.38}$$

The transform components $N_{Re}(z)$, $N_{Im}(z)$ have identical distributions, which means that $\sigma_{N\,\mathrm{Re}}{}^2 = \sigma_{N\,\mathrm{Im}}{}^2$. Therefore:

$$\sigma_{N\,\mathrm{Re}}{}^2 = \sigma_{N\,\mathrm{Im}}{}^2 = \frac{1}{2}\left\langle \left|\tilde{N}(z)\right|^2 \right\rangle = \frac{\eta P_R \tau}{2h\nu_0}\,. \tag{2.39}$$

The probability distribution of the real noise component, which is identical to the imaginary component distribution is calculated to be of the form:

$$P(N_{\mathrm{Re}}) = P_o \exp(-N_{\mathrm{Re}}{}^2 / 2\sigma_{Nre}{}^2)\,. \tag{2.40}$$

The probability distribution of the noise amplitude N(z) is determined from the individual component distributions:

$$\begin{aligned} P(N) &= \int_0^N P(N_{\mathrm{Re}})P(N_{\mathrm{Im}} = \sqrt{N^2 - N_{\mathrm{Re}}{}^2})dN_{\mathrm{Re}} \\ &= \int_0^N P_o{}^2 \exp(-N_{\mathrm{Re}}{}^2 / 2\sigma_{Nre}{}^2)\exp(-(N^2 - N_{\mathrm{Re}}{}^2)/2\sigma_{Nre}{}^2)dN_{\mathrm{Re}} \\ &= \int_0^N P_o{}^2 \exp(-(N^2)/2\sigma_{Nre}{}^2)dN_{\mathrm{Re}}\,. \end{aligned} \tag{2.41}$$

Normalizing the distribution for the noise amplitude:

$$P(N) = \frac{2}{<\left|\tilde{N}(z)\right|^2>} N \exp(-(N^2)/<\left|\tilde{N}(z)\right|^2>)\,. \tag{2.42}$$

Using the probability distribution, the standard deviation of the magnitude of the noise N^2 is calculated:

$$\sigma_{N^2} = \left\langle \left|\tilde{N}(z)\right|^2 \right\rangle = \frac{\eta P_R \tau}{h\nu_0}\,. \tag{2.43}$$

OCT Calculations

Combining all of this analysis, the OCT intensity amplitude, given by the Fourier transform of F(k) is of the form, at $z \neq 0$:

$$\widetilde{I}(z) = I(z)\exp(i\phi(z)) = FT(F(k)) = \widetilde{S}(z) + \widetilde{N}(z)$$

$$= S(z)\exp(i\phi_S(z)) + N(z)\exp(i\phi_N(z)) \,. \tag{2.44}$$

The properties of the signal and noise terms have been derived previously. The magnitude of the OCT intensity can be calculated:

$$\left|\widetilde{\mathrm{I}}(\mathrm{z})\right|^2 = \mathrm{I}(\mathrm{z})^2 = \mathrm{S}(\mathrm{z})^2 + \mathrm{N}(\mathrm{z})^2 - 2\mathrm{S}(\mathrm{z})\mathrm{N}(\mathrm{z})\cos(\phi_S(z) - \phi_N(z)) \,. \tag{2.45}$$

Averaging the OCT intensity, since ϕ_N is completely random:

$$\left\langle \left|\widetilde{\mathrm{I}}(\mathrm{z})\right|^2 \right\rangle = \mathrm{S}(\mathrm{z})^2 + \left\langle \mathrm{N}(\mathrm{z})^2 \right\rangle . \tag{2.46}$$

SNR Definition

System SNR sensitivity definition in OCT is described by the ratio of magnitude of the signal S^2 where the reflection R=1 to the standard deviation of the noise magnitude:

$$\mathrm{SNR_{SDOCT}} = \frac{\mathrm{S}(\mathrm{z},\mathrm{R}=1)^2}{\sigma_{N^2}} = \frac{S^2}{\left\langle \mathrm{N}(\mathrm{z})^2 \right\rangle} = \frac{\left((\eta\tau/h\nu_0)\sqrt{P_R P_S}\right)^2}{(\eta\tau/h\nu_0)P_R} = \frac{\eta P_S \tau}{h\nu_0} \,. \tag{2.47}$$

Compare this to TDOCT SNR of equation (2.18): $\mathrm{SNR_{TDOCT}} = \frac{2\eta' P_S \tau'}{(h\nu_0)}$.

If SDOCT can acquire an entire depth scan (A-scan) in the same time TDOCT acquires one depth location data τ, both techniques will produce comparable SNR. The efficiency of data collection using SDOCT is much greater than that of TDOCT [20,21,22].

2.7 SDOCT Limitations

2.7.1 SDOCT Limitation #1: Mirror Terms in SDOCT

In SDOCT, the OCT intensity is determined by the Fourier transform of the interference fringes measured in k-space:

$$\tilde{I}(z) \approx \sum_j 2\sqrt{P_R P_{Sj}} \int_{-\infty}^{\infty} S(k)\cos(kz_j)\exp(ikz)dk \tag{2.48}$$

The assumption is made that all of the sample reflections are located at longer path lengths than the reference path length, such that $z_j = 2(z_{Sj} - z_R) \geq 0$. Because $\cos(kz_j)$ cannot distinguish between reflections located at $|z_j|$ and $-|z_j|$, all images will experience a mirroring effect over the sample interferometer arm position equal to path length position of the reference arm.

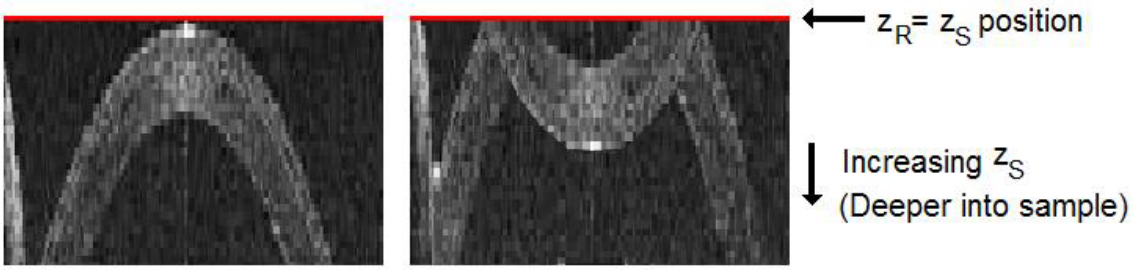

Figure 2.8: Mirroring example of the SDOCT image for two different reference arm positions. The change in the reference arm position of an intensity image (left) creates a mirrored image (right) in this case.

2.7.2 SDOCT Limitation #2: Maximum Imaging Depth in SDOCT

Nyquist theorem defines for a sampling rate of f_0, the maximum resolvable frequency is $f_0/2$. Frequencies of f_0–f are aliased due to limited sampling to a measured frequency of f. The fastest oscillation that can be measured completes a full oscillation in exactly two sampled points.

In terms of k-space measurements of the interference fringes, with an average sampling spacing of δk, the maximum resolvable signal completes a full oscillation within $2\delta k$. With the interference signal $\propto \cos(2k(z_S - z_R))$, the maximum resolvable path length difference of $(z_S - z_R)_{MAX} = \frac{\pi}{2\delta k} = \frac{{\lambda_0}^2}{4\delta\lambda}$ in air, where $\delta k = \frac{2\pi}{{\lambda_0}^2}\delta\lambda$.

2.7.3 SDOCT Limitation #3: SNR Drop with Depth in SDOCT

The spectrometer used in SDOCT creates k-space measurements by integrating over a finite region of k-space. Oscillations in k-space are affected by this finite sampling method. Looking at the interference fringe power measured on the spectrometer at wavenumber k for interference signal $\cos(2k(z_R - z_S))$:

$$P(k) \propto \frac{1}{\delta k}\int_{k-\delta k/2}^{k+\delta k/2}\cos(2k'(z_R - z_S))dk' . \tag{2.49}$$

Using the assumption that $\delta k << k$, the interference measurement can be approximated as:

$$P(k) \propto \cos(2k(z_R - z_S))\left(1 - \frac{\delta k^2 (z_R - z_S)^2}{6}\right). \tag{2.50}$$

Comparing the fringe power amplitude measurement to an ideal case where $\delta k \rightarrow 0$:

$$\frac{P(k)}{P(k, \delta k = 0)} = \left(1 - \frac{\delta k^2 (z_R - z_S)^2}{6}\right). \tag{2.51}$$

This ratio translates to drop in the measured OCT signal over the image depth in SDOCT:

$$\frac{SNR(z = z_R - z_S)}{SNR(z = 0)} = \left(1 - \frac{\delta k^2 (z_R - z_S)^2}{6}\right)^2 . \tag{2.52}$$

In the ideal case, δk in this definition would be the minimum k-space separation of the CCD pixels, designated by δk_{CCD}. In reality, δk is also determined by the ability of the imaging elements to focus an individual wavelength onto each CCD pixel. If the focused spot size of a given wavelength is larger than the CCD pixel, the OCT signal drop will depend on the focused spot size in k-space, designated by δk_{FOCUS}. Assuming that the focused spot size makes the SNR drop over depth dependant on δk_{FOCUS}, the maximum imaging depth is dependant on δk_{CCD}.

Looking at the SNR drop at the maximum imaging depth $(z_S - z_R)_{MAX} = \frac{\pi}{2\delta k_{CCD}} = \frac{{\lambda_0}^2}{4\delta\lambda_{CCD}}$:

$$\frac{SNR(z=(z_R - z_S)_{MAX})}{SNR(z=0)} = \left(1 - \frac{\pi^2}{24}\frac{{\delta k_{FOCUS}}^2}{{\delta k_{CCD}}^2}\right)^2 . \tag{2.53}$$

In terms of wavelength:

$$\frac{SNR(z=(z_R - z_S)_{MAX})}{SNR(z=0)} = \left(1 - 0.41\frac{{\delta\lambda_{FOCUS}}^2}{{\delta\lambda_{CCD}}^2}\right)^2 . \tag{2.54}$$

In the ideal case where the spectrometer measurement is limited by the CCD pixel width, the SNR drop at the maximum depth is calculated:

$$\frac{SNR(z=(z_R - z_S)_{MAX})}{SNR(z=0)} = (1-0.41)^2 = 0.348 = -4.6 \text{ dB}. \tag{2.55}$$

2.8 Phase Changes as Basis of Contrast

As described in Chapter 2.3, the oscillatory portion of the interferometric signal $\cos(2k_0(z_S - z_R))$ can be described by a relative phase $\phi_S - \phi_R$ such that:

$$\cos(2k_0(z_S - z_R)) = \cos(\phi_S - \phi_R) . \tag{2.56}$$

The limitation of the phase is the inability to determine the relative position of the reflections from each interferometer arm beyond an accuracy of $\lambda_0/2$. This results in a phase accuracy limitation of 2π:

$$\phi_S - \phi_R = 4\pi(z_S - z_R)/\lambda_0 + 2\pi m \tag{2.57}$$

where m is an integer to limit the phase measurement to $-\pi \le \phi_S - \phi_R \le \pi$. The cyclic nature of the phase measurements limits the usefulness of the absolute phase measurement of a sample reflection. Changes in the phase measurement can be useful due to the sensitivity to small relative motions occurring between the sample and reference reflections:

$$\Delta\phi = \Delta(\phi_S - \phi_R) = 2k_0\Delta(z_S - z_R) = \frac{4\pi}{\lambda_0}\Delta z\,. \tag{2.58}$$

Due to the cyclic nature of the phase, only phase changes between the limits $-\pi \le \Delta\phi \le \pi$ can be identified properly. Phase changes can identify motions up to a maximum of $\lambda_0/4$, much smaller than the resolution capabilities of the OCT system. The motion calculated by the phase change is only along the axial direction, parallel to the imaging light direction. Using the phase change information of the scatterers within a sample, the tiny motions measured can provide additional contrast to the structural information provided by OCT imaging.

2.8.1 Definition of Phase Noise

With the OCT signal $\tilde{I}(z)$, the calculated phase $\phi(z)$ can deviate from the expected sample phase $\phi_S(z)$ depending on the relative noise properties:

$$\tilde{I}(z) = I(z)\exp(i\phi(z)) = \tilde{S}(z) + \tilde{N}(z) = S(z)\exp(i\phi_S(z)) + N(z)\exp(i\phi_N(z))\,. \tag{2.59}$$

To determine the noise effects on the error on phase measurements, a probability analysis of the phase is required. Since the phase accuracy does not depend on the sample phase, set

$\phi_S(z) = 0$ for convenience. For this case, the phase can be determined through trigonometric means:

$$\tan(\phi(z)) = \frac{N_{\mathrm{Im}}(z)}{S(z) + N_{\mathrm{Re}}(z)}. \tag{2.60}$$

The noise components $N_{Re}(z)$ and $N_{Im}(z)$ have the same Gaussian distribution described earlier. For the case where S >> N, the phase determination can be simplified.

$$\phi(z) \approx \frac{N_{\mathrm{Im}}(z)}{S(z)}. \tag{2.61}$$

The probability distribution of the phase $\phi(z)$ is proportional to the distribution of the noise component, calculated earlier:

$$\mathrm{P}(\varphi) = \mathrm{P}(N_{\mathrm{Im}} = \phi \mathrm{S}) = \mathrm{P}_o \exp(-\phi^2 S^2 / \left\langle \mathrm{N(z)}^2 \right\rangle^2) \tag{2.62}$$

which has a calculated variance of:

$$\sigma_\phi{}^2(z) = \frac{\left|\widetilde{N}(z)\right|^2}{2S(z)^2}. \tag{2.63}$$

Phase error is dependant on the local signal to noise ratio for a given reflector. Phase changes measured for a reflector of OCT signal $S^2(z)$ require two phase measurements, each with phase error associated with it. The phase variance determined for phase changes is twice the value of the error for a single phase measurement:

$$\sigma_{\Delta\phi}{}^2(z) = 2\sigma_\phi{}^2(z) = \frac{\left|\widetilde{N}(z)\right|^2}{S(z)^2} = \frac{1}{SNR(z)}. \tag{2.64}$$

2.9 Choosing Between TDOCT and SDOCT

There are several factors that need to be compared in deciding between TDOCT and SDOCT as the ideal system to produce phase contrast imaging for retinal imaging.

2.9.1 SNR Comparison

Comparing the SNR of 1 pixel in TDOCT to the SNR of an A-scan of SDOCT:

$$\mathrm{SNR_{TDOCT}} = \frac{2\eta_{TD} P_S \tau_{TD}}{h\nu_0}, \mathrm{SNR_{SDOCT}} = \frac{\eta P_S \tau}{h\nu_0}. \quad (2.65)$$

It can be approximated that $SNR_{TDOCT} \approx SNR_{SDOCT}$ when the acquisition time of 1 depth location in TDOCT matches the acquisition time of an entire depth scan in SDOCT. With such a large improvement of image acquisition efficiency, SDOCT is the optimum choice in general.

2.9.2 Phase measurements with TDOCT versus SDOCT

SDOCT intrinsically measures the phase from all of the depth reflections at the same time. Any unwanted bulk axial motion of the sample can be analyzed and removed from contrast measurements. TDOCT has only one measurement of phase for each pixel acquired. If bulk sample motion removal is required, additional hardware and analysis would be required in the TDOCT system to measure a reference phase for removal. With the ease of simultaneously acquiring the phases from all of the sample depths, SDOCT is the optimum choice under this regard.

2.9.3 Spectral shaping and Dispersion compensation

As described in Chapter 2.2, optimal imaging in OCT depends on the shape of the coherence function. The width of the function determines the axial resolution, while the shape and side lobes of the function determine the image artifacts created by strong reflections within the sample. Another factor which determines the shape of the coherence function is the relative dispersion between the optical paths of the interferometer arms in the system. Mismatches between sample and reference interferometer arms can broaden and distort the coherence function, reducing image quality.

Variations in the dispersion properties of different samples can ultimately limit the axial resolution without any further adjustment to the system dispersion. SDOCT can numerically compensate for dispersion mismatches between the interferometer arms as well as adjust the spectral shape to improve the coherence function shape. TDOCT can only alter these factors through optical adjustment to the system.

2.9.4 Minimum time required per transverse location

The minimum time per transverse location in SDOCT is determined by the acquisition rate of the spectrometer camera, which is limited by currently available commercial technologies. TDOCT can theoretically achieve a much faster acquisition rate of each pixel for currently available hardware. If faster acquisition speeds are required than can be achieved with SDOCT, TDOCT is the only available option to meet those requirements.

2.9.5 Limitations of SDOCT

Considering all of the limitations of SDOCT described in Chapter 2.7, proper optical alignment of the thin retinal sample can reduce most of the negative effects of these limitations.

Unless the OCT imaging situation requires a transverse pixel dwell time shorter than SDOCT is capable of, SDOCT has comparable or superior performance to TDOCT and is clearly the optimal choice for proceeding with phase contrast imaging.

2.10 References

1. D. Huang et al., “Optical coherence tomography,” Science 254, 1178 (1991).
2. W. Drexler et al., “In vivo ultrahigh resolution optical coherence tomography,” Opt. Letters 24, 1221 (1999).
3. Z. Yaqoob et al., “Homodyne en face optical coherence tomography,” Opt. Letters 31, 1815 (2006), http://www.opticsinfobase.org/abstract.cfm?URI=ol-31-12-1815.
4. B. Hoeling et al., “Phase modulation at 125kHz in a Michelson interferometer using an inexpensive piezoelectric stack driven at resonance,” Rev. Sci. Instr. 72, 1630 (2001).

5. M. Pircher et al., “Retinal cone mosaic imaged with transverse scanning optical coherence tomography,” Opt. Letters 31, 1821-1823 (2006).
6. K. Grieve et al., “Ocular tissue imaging using ultrahigh-resolution, full-field optical coherence tomography,” Invest. Ophthalmol. Vis. Sci. 45, 4126 (2004).
7. R.G. Cucu et al., “Combined confocal/en face T-scan based ultrahigh-resolution optical coherence tomography in vivo retinal imaging,” Opt. Letters 31, 1684 (2006)
8. B. Bouma, E. Tearney, Handbook of Optical Coherence Tomography, (Marcel Dekker, Inc., 2002).
9. A.F. Fercher et al., “Measurement of intraocular distances by backscattering spectral interferometry,” Opt. Commun. 117, 43 (1995).
10. M. Wojtkowski et al., ”In vivo human retinal imaging by fourier domain optical coherence tomography,” J. Biomed. Opt. 7, 457-463 (2002).
11. R. Leitgeb et al., “Ultrahigh resolution Fourier domain optical coherence tomography,” Opt. Express 12, 2156 (2004). http://www.opticsexpress.org/abstract.cfm?id=79930.
12. S. R. Chinn et al., “Optical coherence tomography using a frequency-tunable optical source,” Opt. Letters 22, 340-342 (1997).
13. B. Golubovic et al., “Optical frequency-domain reflectometry using rapid wavelength tuning of a Cr4+:forsterite laser,” Opt. Letters 22, 1704-1706 (1997).
14. E. C. Lee et al., “In vivo optical frequency domain imaging of human retina and choroid,” Opt. Express 14, 4403-4411 (2006), http://www.opticsexpress.org/abstract.cfm?id=89920.
15. H. Lim et al., “Optical frequency domain imaging with a rapidly swept laser in the 815-870 nm range,” Opt. Express 14, 5937-5944 (2006), http://www.opticsexpress.org/abstract.cfm?id=90546.
16. R. Huber et al., “Amplified, frequency swept lasers for frequency domain reflectometry and OCT imaging: design and scaling principles,” Opt. Express 13, 3513-3528 (2005), http://www.opticsexpress.org/abstract.cfm?&id=83745.
17. “Line Scan Cameras,” Basler Vision Technologies, http://www.baslerweb.com/beitraege/beitrag_en_17842.html.
18. “CCD Monochrome Linescan Cameras,” Atmel Corporation, http://www.atmel.com/dyn/products/devices.asp?family_id=612.
19. “Line Scan Cameras,” DALSA, http://vfm.dalsa.com/products/linescan.asp.
20. M. Choma et al., “Sensitivity advantage of swept source and Fourier domain optical coherence tomography,” Opt. Express 11, 2183-2189 (2003), http://www.opticsinfobase.org/abstract.cfm?URI=oe-11-18-2183.
21. R. Leitgeb et al., “Performance of fourier domain vs. time domain optical coherence tomography,” Opt. Express 11, 889-894 (2003), http://www.opticsinfobase.org/abstract.cfm?URI=oe-11-8-889.
22. J. F. de Boer et al., “Improved signal-to-noise ratio in spectral-domain compared with time-domain optical coherence tomography,” Opt. Letters 28, 2067-2069 (2003).